第 43 卷 第 1 期/2023 年 1 月/光学学报 研究论文

光学学报

近红外磁表面等离激元单向波导

严金华，王琳萍，邓羽析，刘博云，沈林放*

浙江工业大学理学院，浙江 杭州 310023

摘要 基于电介质-旋电介质的磁表面等离激元(SMPs)模型，从色散方程出发，理论分析了存在表面波时旋电介质介电张量和电介质介电系数的关系，以实现单向传输的SMPs。提出Ce:YIG/Ag超构旋电材料，根据有效介电张量理论构造满足SMPs条件的旋电介质的介电张量。分析了电介质-旋电介质表面波的色散特性，利用有限元方法对电介质-超构旋电介质模型的传输特性进行了仿真计算，在施加常规磁场(0.2 T)情况下实现了工作于近红外波段的SMPs单向传输，并在该结构中引入缺陷。仿真结果表明该SMPs单向波导具有很好的鲁棒性。

关键词 表面光学；磁表面等离激元；单向电磁模式；超构材料；近红外；有限元方法

中图分类号 O436 **文献标志码** A **DOI**：10.3788/AOS221080

1 引 言

单向电磁模式是通过打破洛伦兹互易性实现沿一个方向传输而不会沿原路径返回的电磁模式，其具有无反向散射的特性，在激光和光通信系统[1-2]、隔离器[3]、环行器[4]等方面有广泛应用。在由磁光材料构成的波导系统中，通过引入磁场可打破时间反演对称，进而可实现单向电磁模式。一种方法是利用光子晶体中类似量子霍尔边缘态构造单向电磁模式[5-8]，内部光子禁带使得电磁模式只能在边缘传输，引入外磁场可打破时间反演对称性，实现单向电磁模式，这一现象在磁光光子晶体中得到实验验证[9-10]。另一种方法是利用磁表面等离激元(SMPs)实现单向模式，该模式存在于旋电介质和电介质之间的界面，施加外磁场使得正反两个方向波矢的色散曲线分离[11]，当频率处于色散曲线频率间隙内时电磁波可以单向传播，单向频带范围可通过调谐磁场来实现单向电磁模式[12]。相比前一种方法，基于SMPs的单向模式结构更加简单，且能够将光束约束在表面，并具有较好的鲁棒性[13]，对器件小型化以及光通信领域应用[14]有重要意义。

利用SMPs实现光波段和微波段单向电磁模式一直是研究的热点[15-16]。2008年，Fan团队[15]利用光子晶体的禁带抑制体模，在光子晶体和金的界面上实现光波段的单向表面波，但由于在光波段使金产生旋电效应所需的磁场非常强(约10^4 T)，从而限制了其应用。2015年，Shen等[16]将目光转向太赫兹波段，利用半导体材料InSb和电介质构建了三明治结构，该结构在常规磁场大小情况下实现了单向SMPs。单向SMPs为功能器件提供了传播方向和频率范围等方面的更多设计自由度，如可通过构建紧凑圆形腔实现环形器[17]。在光波段且在常规大小磁场下，一般磁光材料的磁场导致的介电张量非对角项与对角项比值仅约为10^{-3}[18]，产生具有单向传输特性的边缘态或SMPs均较为困难。为解决这一问题，Kempa团队[19]利用金属和旋电介质组合形成超构材料，并在其中构造光子晶体禁带以实现光波段的边缘态单向传输。

本文在介电材料和旋电材料构成的模型中，根据表面波存在的条件，在常规磁场大小(0.2 T)情况下构造超构材料并得到满足表面波条件的介电张量，分析了SMPs的色散条件，针对1.1 eV波段仿真实现了单向表面波，通过在界面上引入缺陷仿真分析了单向传输的鲁棒性。

2 基本模型和理论

2.1 基本模型

考虑一个由旋电材料和介电材料构成的界面，如图1所示。光波沿x方向传播，介电材料和旋电材料分别位于$y>0$和$y<0$的半无限空间，在z方向上无限延伸。介电材料的介电系数为ε_d。沿z方向施加大小为B_0的磁场，在外磁场的作用下，旋电材料的介电系数可表示为张量形式[11]：

$$\varepsilon_g=\begin{pmatrix}\varepsilon_1 & \mathrm{i}\varepsilon_2 & 0\\ -\mathrm{i}\varepsilon_2 & \varepsilon_1 & 0\\ 0 & 0 & \varepsilon_3\end{pmatrix},\tag{1}$$

收稿日期：2022-05-09；**修回日期**：2022-06-04；**录用日期**：2022-07-04；**网络首发日期**：2022-07-14

基金项目：国家自然科学基金(62075197，62101496)

通信作者：*lfshen@zjut.edu.cn

式中：i为虚数单位；在没有外磁场的情况下，$\varepsilon_1=\varepsilon_3$，$\varepsilon_2=0$。在外磁场作用下，磁光材料表现出旋电效应，在介电张量中产生非互易张量元素ε_2，通常用来表征磁光效应的强弱。

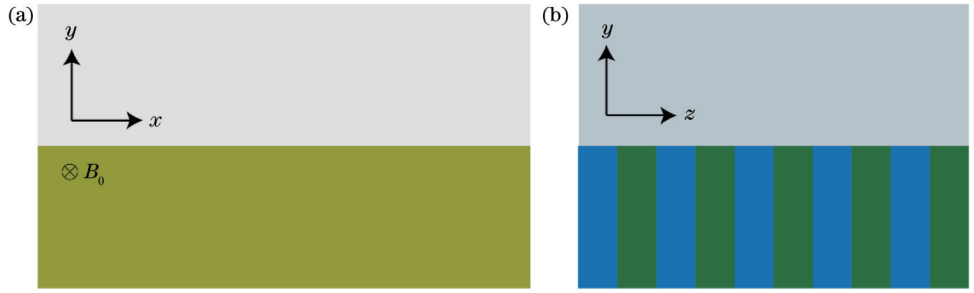

图1　单向SMPs波导模型。(a) x-y平面结构图；(b) y-z平面结构图

Fig. 1　Physical models of unidirectional waveguide based on SMPs. (a) Structural diagram in x-y plane; (b) structural diagram in y-z plane

2.2　理论条件

SMPs中的电磁模式为横磁(TM)模，由界面处电磁场分量的连续性条件可以得到色散方程[11]：

$$\alpha_g+\alpha_d\frac{\varepsilon_{gv}}{\varepsilon_d}-\frac{\varepsilon_2}{\varepsilon_1}k=0, \tag{2}$$

式中：$\alpha_d=\sqrt{k^2-\varepsilon_d k_0^2}$，$k_0=\omega/c$（$\omega$和$c$分别为角频率和真空中光速）为真空中的波数；$\alpha_g=\sqrt{k^2-\varepsilon_{gv}k_0^2}$分别是光波在介电材料和旋电材料中垂直于界面的波数；$\varepsilon_{gv}=\varepsilon_1\left(1-\varepsilon_2^2/\varepsilon_1^2\right)$为Voigt系数；$k$为SMPs沿着界面的波数。

将上述系数表达式代入色散方程[式(2)]，实际上得到一个关于k的一元四次方程$k^4\left[\left(\varepsilon_d/\varepsilon_1+\varepsilon_{gv}/\varepsilon_d\right)^2-4\right]+k^2k_0^2\left[4\left(\varepsilon_d+\varepsilon_{gv}\right)-2\left(\varepsilon_d/\varepsilon_1+\varepsilon_{gv}/\varepsilon_d\right)\left(\varepsilon_d+\varepsilon_{gv}\right)\right]+k_0^4\left[\left(\varepsilon_d+\varepsilon_{gv}\right)^2-4\varepsilon_d\varepsilon_{gv}\right]=0$，若以$k^2$为变量，则得到一元二次方程。如果存在表面波，该一元二次方程应当存在解，根据一元二次方程解的存在条件，可以得到该一元二次方程中各介电系数的关系。由于模型的上层材料为介电材料，故$\varepsilon_d>0$。为简化表述，令$y=\varepsilon_2^2/\varepsilon_1^2$，$x=\varepsilon_1/\varepsilon_d$，得到式(2)存在解的条件为

$$\left(1/x+1\right)^2<y<\left(1/x-1\right)^2。 \tag{3}$$

由于SMPs要求旋电材料介电张量的对角项$\varepsilon_1<0$，故$x<0$。上层介质以PMMA材料为例，$\varepsilon_d=2.28$[20]，将式(3)中x和y的取值范围作图，如图2所示，实线和虚线之间的区域即SMPs存在的范围。考虑一般旋电磁光材料，张量中ε_2的取值取决于磁场大小和材料本身特性，且数值远小于ε_1，导致y的取值接近于0，即图2中$x\approx-1$（$|\varepsilon_1|$与ε_d大小接近）。

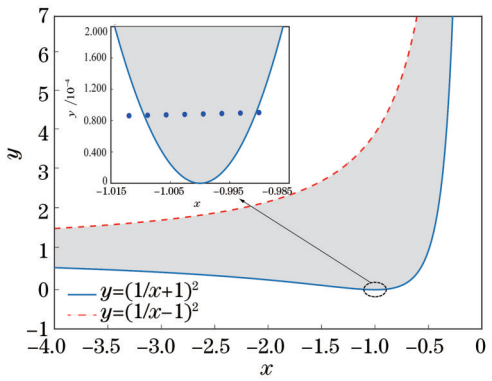

图2　存在SMPs的范围($\varepsilon_d=2.28$)，插图为虚线圆圈内的放大图，插图内的圆点为不同比例时所对应的x和y值(比例因子p_m从0.1076至0.1083的取值间隔0.0001)

Fig. 2　Range for existence of SMPs ($\varepsilon_d=2.28$) [inset is enlarged view of region in dashed circle, and dots in inset correspond different ratios (scaling factor p_m is from 0.1076 to 0.1083 at interval of 0.0001)]

3　模型构造与特性分析

3.1　模型有效介电张量

根据式(2)和图2，旋电介质介电张量中的对角分量和非对角分量满足条件时，可以得到单向SMPs。然而，单一磁光介质的介电张量很难满足这个条件范围。可通过构造超构材料获得满足上述条件的介电张量。掺铈钇铁石榴石(Ce:YIG)在近红外波段具有低吸收特性，且在常规大小磁场(0.2 T)下可获得较大的非对角介电系数[21]，这对于设计非互易集成光子器件具有重要意义。在1.1 eV频率处，Ce:YIG的介电张量非对角项达到最大，其介电张量为

$$\varepsilon_y=\begin{pmatrix}5.4 & 0.024\mathrm{i} & 0\\ -0.024\mathrm{i} & 5.4 & 0\\ 0 & 0 & 5.4\end{pmatrix}。 \tag{4}$$

根据有效介电张量理论[22]，引入介电系数为负数的金属，将其与Ce:YIG交替组成超构材料，如图1(b)所示，以降低超构材料介电张量的对角项分量，即式(1)中的ε_1。银(Ag)是一种在近红外波段常用的金属材料，在工作频率为1.1 eV时介电系数$\varepsilon_m=-65.765$[23]。在常规大小磁场下，磁场导致的介

电张量非对角项可以忽略不计，可认为是各向同性介质，介电张量可表示为

$$\varepsilon_{\mathrm{m}}=\begin{pmatrix}-65.765 & 0 & 0\\ 0 & -65.765 & 0\\ 0 & 0 & -65.765\end{pmatrix}。\tag{5}$$

Ag 和 Ce∶YIG 组成的超构材料的介电张量元素[22]可表示为

$$\begin{cases}\varepsilon_{\mathrm{g1}}=p_{\mathrm{m}}\varepsilon_{\mathrm{m1}}+p_{\mathrm{y}}\varepsilon_{\mathrm{y1}}\\ \varepsilon_{\mathrm{g2}}=p_{\mathrm{m}}\varepsilon_{\mathrm{m2}}+p_{\mathrm{y}}\varepsilon_{\mathrm{y2}}\\ 1/\varepsilon_{\mathrm{g3}}=p_{\mathrm{m}}/\varepsilon_{\mathrm{m3}}+p_{\mathrm{y}}/\varepsilon_{\mathrm{y3}}\end{cases},\tag{6}$$

式中：下标 m 和 y 分别表示 Ag 和 Ce∶YIG，g 表示组合得到的超构旋电材料；p_{m} 和 $p_{\mathrm{y}}=1-p_{\mathrm{m}}$ 分别为 Ag 和 Ce∶YIG 两种材料的比例因子；下角标 1、2、3 所对应的介电系数与式(1)中 ε_1、ε_2 和 ε_3 的含义相同。超构旋电材料的介电张量各项值随着比例因子 p_{m} 值的改变而改变。上层介电材料 PMMA 的介电系数 $\varepsilon_{\mathrm{d}}=2.28$[20]，改变 Ag 的比例因子 p_{m}，得到不同的 x 和 y 值。图 2 插图中的圆形实心点为 p_{m} 不同取值所对应的 x 和 y 坐标，p_{m} 从 0.1076 到 0.1083 的取值间隔为 0.0001，对应从右到左的圆形实心点。只有处于图 2 中阴影区域范围内的取值，才满足 SMPs 条件。

以 $p_{\mathrm{m}}=0.108$、$p_{\mathrm{y}}=0.892$ 为例，在频率为 1.1 eV 时，Ag 和 Ce∶YIG 组合得到的超构材料介电张量为

$$\varepsilon_{\mathrm{g}}=\begin{pmatrix}-2.286 & 0.0214\mathrm{i} & 0\\ -0.0214\mathrm{i} & -2.286 & 0\\ 0 & 0 & 6.115\end{pmatrix}。\tag{7}$$

超构材料的介电张量会随着组分比例的变化而变化，即使在组分比例确定的情况下，由于组成超构材料的 Ce∶YIG[21] 和 Ag[23] 在近红外波段具有色散特性，因此超构材料的介电张量也会相应地发生变化，PMMA 的介电系数可视作不变。在 $p_{\mathrm{m}}=0.108$、$p_{\mathrm{y}}=0.892$ 这一组分比例情况下，根据 Ce∶YIG 和 Ag 在 1.1 eV 频率附近的色散参数可得超构材料的色散特性，利用式(2)可得到 SMPs 的色散曲线，如图 3 所示。很明显，

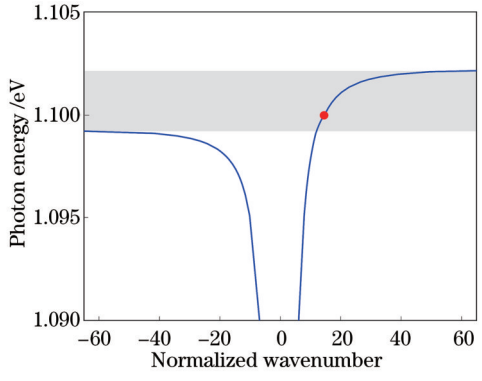

图 3　光子能量为 1.1 eV 附近的 SMPs 色散曲线(圆点对应的光子能量为 1.1 eV)

Fig. 3　SMPs dispersion curve for photon energy around 1.1 eV (dot corresponds to photon energy of 1.1 eV)

由于旋电材料介电张量非对角项的存在，随着频率的增加，$k>0$ 和 $k<0$ 两个方向的波数呈现不同的特性，电磁波的色散曲线产生分离，即存在一个单向传输频率带隙，在这个频率带隙内，只存在正向传播的电磁波，处于这个单向频率带隙外的电磁波不满足单向传播条件。图 3 中圆点对应的频率为 1.1 eV，是本文进行单向特性仿真的频率。

3.2　SMPs 传输特性

使用有限元仿真软件 COMSOL Multiphysics 对图 1 所示模型进行了仿真模拟。上层介电材料的介电常数为 $\varepsilon_{\mathrm{d}}=2.28$，厚度为 $d=100$ nm；下层超构旋电材料的介电张量如式(7)所示，厚度 $h=150$ nm。以磁流源为激励源，工作频率为 1.1 eV。激励源位于界面上 $L/2$(L 为波导沿着传输界面的长度)处时，得到的结果如图 4(a)所示。改变磁场方向，SMPs 单向传输方向也发生改变，如图 4(b)所示。图 4(d)为图 4(a)虚线处的电场分布，SMPs 在垂直于材料界面方向上呈指数衰减，从图中数据可知电介质层和超构材料层的穿透深度分别为 $\hat{y}_{\mathrm{d}}=13$ nm 和 $\hat{y}_{\mathrm{g}}=12.9$ nm，即 SMPs 被限制在介电材料和超构材料的界面上。根据 $\hat{y}_{\mathrm{d}}=1/\alpha_{\mathrm{d}}$ 和 $\hat{y}_{\mathrm{g}}=1/\alpha_{\mathrm{g}}$，理论求得在该工作频率下电介质层和超构材料层的穿透深度分别为 $\hat{y}_{\mathrm{d}}=13.02$ nm 和 $\hat{y}_{\mathrm{g}}=12.87$ nm。由于 $\varepsilon_{\mathrm{gv}}<0$ 且 $\varepsilon_{\mathrm{d}}>0$，所以 $\hat{y}_{\mathrm{d}}>\hat{y}_{\mathrm{g}}$，理论计算和仿真得到的结果相符。将激励源偏离界面放置，置于界面下方 20 nm 处，激发得到的电场模式仍然束缚在界面并具有单向传输特性，如图 4(c)所示，表明该模型对表面波具有非常强的束缚性。

图 4(e)为图 4(a)中沿着界面的电场强度分布，可以很明显地看出：反向传输的方向上电场强度迅速衰减，几乎不存在反向散射传输的表面波，即该结构对反向散射免疫。由于反向传输的电场在非常短的距离(小于半个波长)内得到抑制，因此可以用于设计亚波长尺寸的光隔离器，这对于提高光子集成度具有重要意义。这种单个界面的结构兼容现有的集成光学制备工艺，下层的旋电材料为层叠超构结构，可在衬底上通过镀膜、光刻等工艺进行制备，上层介电材料可通过旋涂有机介质或者沉积二氧化硅实现。

为验证基于 SMPs 的单向波导对于界面缺陷具有鲁棒性，在界面上设置突起与凹陷。在 $2L/3$ 处放置半径 $R=12$ nm 的圆，图 5(a)中圆形内材料设置与下层超构材料一致，表示传输界面上设置突起，图 5(b)中圆形内材料设置与上层电介质一致，表示传输界面上设置凹陷。结果表明：SMPs 在遇到缺陷障碍物时会绕过障碍物并继续传输。图 5(c)和图 5(d)分别是与图 5(a)和图 5(b)相对应地在传输方向电介质与超构材料界面上的电场幅度分布，与不设置缺陷的电场幅度分布比较，尽管在设置缺陷处电场幅度发生剧烈振荡，但表面波在绕过缺陷后迅速回到界面上，并恢复到原来的幅度

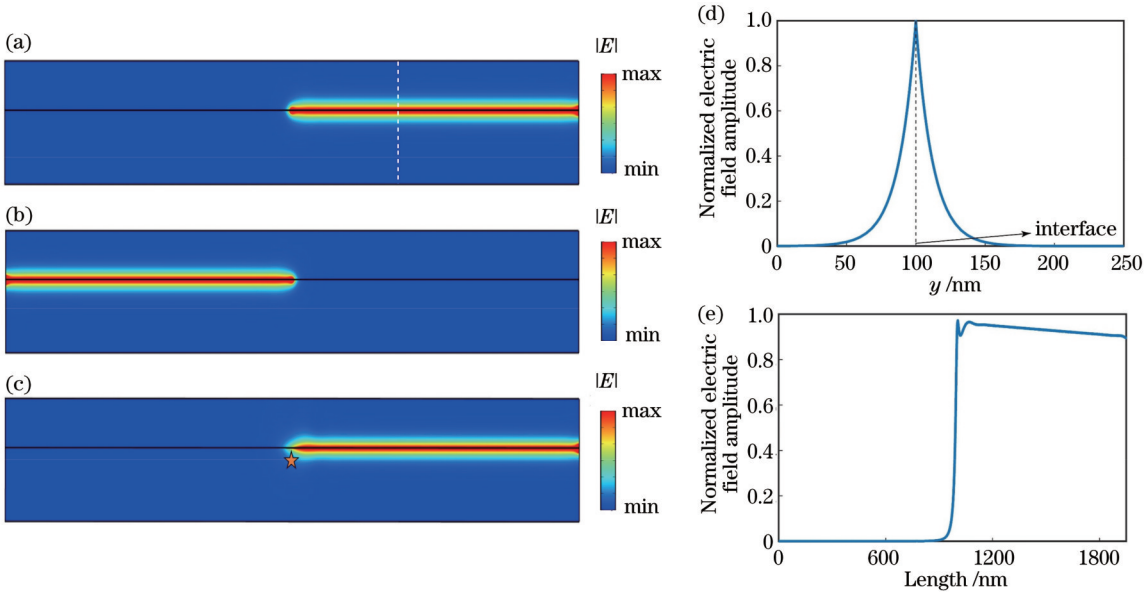

图 4　SMPs 电场强度分布。(a)磁场方向为 $-z$ 方向;(b)磁场方向为 $+z$ 方向;(c)激励源放置在界面下方 20 nm(五角星处);(d)图 4(a)虚线处的归一化电场强度分布;(e)图 4(a)中沿着界面的归一化电场强度分布

Fig. 4　Distributions of electric field amplitudes of SMPs. (a) Direction of magnetic field towards $-z$ direction; (b) direction of magnetic field towards $+z$ direction; (c) source is placed inside gyroelectric material, 20 nm below interface (at position of star); (d) normalized electric field amplitude at dashed line in Fig. 4(a); (e) normalized electric field amplitude along interface in Fig. 4(a)

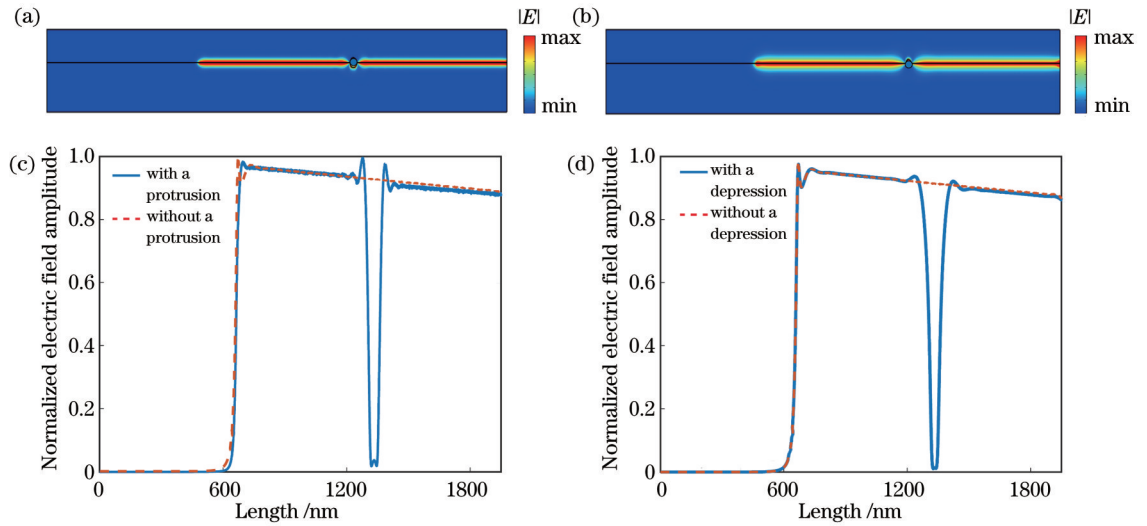

图 5　SMPs 的鲁棒性。(a)传输界面上存在突起;(b)传输界面上存在凹陷;(c)与图 5(a)对应的传输方向上归一化电场强度;(d)与图 5(b)对应的传输方向上归一化电场幅度

Fig. 5　Robustness of SMPs. (a) There is protrusion on transport interface; (b) there is depression on transport interface; (c) normalized electric field amplitude in transmission direction corresponding to Fig. 5(a); (d) normalized electric field amplitude in transmission direction corresponding to Fig. 5(b)

大小,几乎没有产生能量损失。这表明单向波导具有很好的鲁棒性,界面缺陷不影响表面波的传输,也不影响单向传输特性,这一特性可以降低光子器件制造过程中的工艺要求。

基于 SMPs 的单向波导不仅对于缺陷具有很好的鲁棒性,对于大角度弯曲波导也有非常好的通过性。考虑 SMPs 通过一直角波导,如图 6 所示,台阶高度为 150 nm,长度为 800 nm,整个模型的宽度 $L=2000$ nm,磁流源放置在 $x=400$ nm 处。结果表明:SMPs 沿着材料的界面进行传输,并顺着界面“爬”上台阶,在通过 4 个直角后被继续很好地约束在界面处传播,没有引入背向散射,这是普通的波导所不具备的性质,为在亚波长结构中操控“光”和设计复杂结构的光器件提供了便利。

4　结　　论

从电介质/旋电材料界面的 SMPs 色散方程出发,

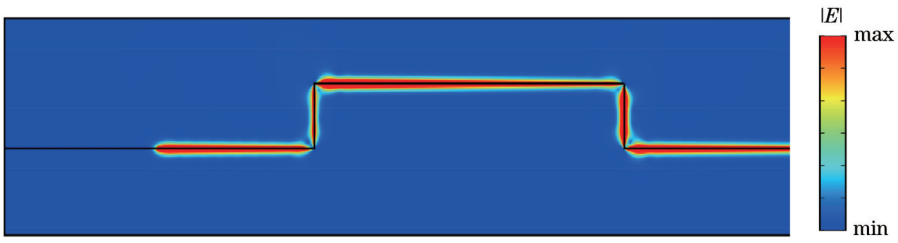

图 6 SMPs在经过90°波导时电场幅度分布图

Fig. 6 Distribution of electric field amplitude of SMPs passing through 90° waveguide

分析探讨了方程有解即表面波存在的条件，得到存在SMPs时旋电介质介电张量应满足的条件。根据这一条件和有效介电张量理论，提出利用Ag/Ce∶YIG复合材料构建满足条件的旋电介质的介电张量，基于这一方法可以构造在常规磁场大小情况下工作于近红外波段的SMPs单向波导，并分析了其色散特性，色散曲线表明这种结构存在单向传输频率带隙。在近红外单向频段内，仿真计算了单向传输特性，SMPs在经过界面缺陷时能很快恢复到原来的电场强度且几乎没有能量损失，这说明基于该结构模型的单向表面波还具有很好的鲁棒性，界面缺陷不影响表面波的传输和单向特性。该结构可在亚波长尺寸内完全抑制反向散射，可以用于设计亚波长尺寸的光隔离器。

参 考 文 献

[1] Asadchy V S, Mirmoosa M S, Díaz-Rubio A, et al. Tutorial on electromagnetic nonreciprocity and its origins[J]. Proceedings of the IEEE, 2020, 108(10): 1684-1727.

[2] Caloz C, Alù A, Tretyakov S, et al. Electromagnetic nonreciprocity[J]. Physical Review Applied, 2018, 10(4): 047001.

[3] Wang C, Zhong X L, Li Z Y. Linear and passive silicon optical isolator[J]. Scientific Reports, 2012, 2: 674.

[4] Jalas D, Petrov A, Eich M, et al. What is, and what is not, an optical isolator[J]. Nature Photonics, 2013, 7(8): 579-582.

[5] Haldane F D M, Raghu S. Possible realization of directional optical waveguides in photonic crystals with broken time-reversal symmetry[J]. Physical Review Letters, 2008, 100(1): 013904.

[6] Marqués R, Martel J, Mesa F, et al. Left-handed-media simulation and transmission of EM waves in subwavelength split-ring-resonator-loaded metallic waveguides[J]. Physical Review Letters, 2002, 89(18): 183901.

[7] Chen J J, Li Z, Yue S, et al. Efficient unidirectional generation of surface plasmon polaritons with asymmetric single-nanoslit[J]. Applied Physics Letters, 2010, 97(4): 041113.

[8] 李雪梅, 张明达, 朱小冬, 等. 光通信波段中基于谷霍尔效应的单向波导[J]. 光学学报, 2021, 41(19): 1913001.
Li X M, Zhang M D, Zhu X D, et al. Unidirectional wave guide based on valley Hall effect in optical communication band[J]. Acta Optica Sinica, 2021, 41(19): 1913001.

[9] Wang Z, Chong Y D, Joannopoulos J D, et al. Observation of unidirectional backscattering-immune topological electromagnetic states[J]. Nature, 2009, 461(7265): 772-775.

[10] 陈剑锋, 梁文耀, 李志远. 磁光光子晶体中拓扑光子态研究进展[J]. 光学学报, 2021, 41(8): 0823015.
Chen J F, Liang W Y, Li Z Y. Progress of topological photonic state in magneto-optical photonic crystal[J]. Acta Optica Sinica, 2021, 41(8): 0823015.

[11] Brion J J, Wallis R F, Hartstein A, et al. Theory of surface magnetoplasmons in semiconductors[J]. Physical Review Letters, 1972, 28(22): 1455-1458.

[12] Hu B, Wang Q J, Zhang Y. Broadly tunable one-way terahertz plasmonic waveguide based on nonreciprocal surface magneto plasmons[J]. Optics Letters, 2012, 37(11): 1895-1897.

[13] 张羊羊, 朱方明, 沈林放, 等. 介质填充浅槽周期结构表面上的太赫兹表面等离子体激元[J]. 光子学报, 2012, 41(4): 389-393.
Zhang Y Y, Zhu F M, Shen L F, et al. Terahertz surface plasmon polaritons on metal surfaces corrugated by shallowly dielectric-filled grooves[J]. Acta Photonica Sinica, 2012, 41(4): 389-393.

[14] 王琳, 张磊. 基于表面等离激元谐振腔的窄谱增强传感器[J]. 光学学报, 2021, 41(7): 0724001.
Wang L, Zhang L. Narrow-spectrum enhanced sensor based on surface plasmon resonator[J]. Acta Optica Sinica, 2021, 41(7): 0724001.

[15] Yu Z F, Veronis G, Wang Z, et al. One-way electromagnetic waveguide formed at the interface between a plasmonic metal under a static magnetic field and a photonic crystal[J]. Physical Review Letters, 2008, 100(2): 023902.

[16] Shen L F, You Y, Wang Z Y, et al. Backscattering-immune one-way surface magnetoplasmons at terahertz frequencies[J]. Optics Express, 2015, 23(2): 950-962.

[17] Liu K X, Torki A, He S L. One-way surface magnetoplasmon cavity and its application for nonreciprocal devices[J]. Optics Letters, 2016, 41(4): 800-803.

[18] Wang Z, Chong Y D, Joannopoulos J D, et al. Reflection-free one-way edge modes in a gyromagnetic photonic crystal[J]. Physical Review Letters, 2008, 100(1): 013905.

[19] Wu X Y, Ye F, Merlo J M, et al. Topologically protected photonic edge states in the visible in plasmo-gyroelectric metamaterials[J]. Advanced Optical Materials, 2018, 6(15): 1800119.

[20] Beadie G, Brindza M, Flynn R A, et al. Refractive index measurements of poly(methyl methacrylate) (PMMA) from 0.4–1.6 μm[J]. Applied Optics, 2015, 54(31): F139-F143.

[21] Onbasli M C, Beran L, Zahradník M, et al. Optical and magneto-optical behavior of Cerium Yttrium Iron Garnet thin films at wavelengths of 200–1770 nm[J]. Scientific Reports, 2016, 6: 23640.

[22] Bergman D J. The dielectric constant of a composite material: a problem in classical physics[J]. Physics Reports, 1978, 43(9): 377-407.

[23] Johnson P B, Christy R W. Optical constants of the noble metals [J]. Physical Review B, 1972, 6(12): 4370-4379.

Near-Infrared Unidirectional Waveguide Based on Surface Magnetoplasmons

Yan Jinhua, Wang Linping, Deng Yuxi, Liu Boyun, Shen Linfang*

College of Science, Zhejiang University of Technology, Hangzhou 310023, *Zhejiang, China*

Abstract

Objective Unidirectional electromagnetic mode travels along one direction and immunes from backscattering by breaking Lorentz reciprocity. As free from backscattering, it is widely used in laser and optical communication systems. In addition, the unidirectional electromagnetic mode can be realized by introducing a magnetic field to break the time inversion symmetry. The most promising method to realize a unidirectional electromagnetic mode is to use surface magnetoplasmons (SMPs) which exist in the interface between the gyro-electric and dielectric media, and an external magnetic field can be applied to separate the dispersion curves of wave vectors in both directions. When the frequency falls into the gap of the dispersion curves, the electromagnetic wave propagates in one direction. In terahertz bands, achievements on an SMPs-based unidirectional electromagnetic mode are reported in terms of the interface of the semiconductor InSb and the dielectric medium with a normal magnetic field magnitude. While in near-infrared bands, it is difficult to produce SMPs by using magneto-optical materials since the ratio of the non-diagonal term to the diagonal term of the dielectric tensor under the normal magnetic field magnitude is only about 10^{-3}. In order to solve this problem, a meta-material is employed to enhance the ratio of the non-diagonal term to the diagonal term of the dielectric tensor, and SMPs in a 1.1 eV band are achieved at the interface of the proposed meta-material and the dielectric material.

Methods A physical model of a unidirectional waveguide based on SMPs was presented in this paper. The model is an interface consisting of meta-material-based gyro-electric and dielectric materials (PMMA, with a dielectric coefficient of 2.28). According to the continuity condition, a dispersion equation was obtained. The relationship between the dielectric tensor of the gyro-dielectric material and the dielectric coefficient was theoretically analyzed when SMPs existed. Since the non-diagonal term of the dielectric tensor of normal magneto-optical materials is much smaller than the diagonal term, the diagonal term of the dielectric tensor of the meta-material-based gyro-electric materials is close to the dielectric coefficient of the dielectric materials. In order to construct meta-material-based gyro-electric materials, cerium-doped yttrium iron garnet (Ce∶YIG) and silver with a negative dielectric coefficient were employed. Due to the low absorption and large non-diagonal dielectric coefficient under the normal magnitude of magnetic field (0.2 T), Ce∶YIG was widely used in the near-infrared bands. According to the effective dielectric tensor theory, the dielectric tensor of the meta-material-based gyro-electric materials with different proportions could be obtained. With a ratio of 0.108/0.892 (Ag/Ce∶YIG), the dispersion curves of the SMPs were given, from which it is obvious that the unidirectional band exists around a frequency of 1.1 eV.

Results and Discussions The characteristics of unidirectional propagation were simulated and analyzed in this paper. The electric field distribution along the interface is shown in Fig. 4 by placing an excitation source in the interface. The electric field rapidly decays in the opposite direction, and there is almost no backscattering. In other words, the structure is immune to backscattering. Since the electric field in the opposite direction is suppressed within a distance of less than half a wavelength, it can be used to design optical isolators in sub-wavelength size, which is of great significance for improving photonic integration. By setting protrusions and depressions on the interface, the robustness of the unidirectional waveguide to interface defects is verified. As shown in Fig. 5, although the electric field amplitude oscillates violently at the setup defect, the surface wave quickly returns to the interface after bypassing the defect and converts back into its original amplitude size with little energy loss. It shows that the unidirectional waveguide has good robustness as the interface defects do not affect the transmission of surface waves or weaken the unidirectional transmission characteristics. This property is helpful to reduce the process requirements during the manufacturing of photonic devices. SMPs-based unidirectional waveguides not only show positive robustness to defects but also have excellent unidirectional characteristics for waveguides with large-angle bending. Fig. 6 shows the transmission characteristics of a structure at four right angles, and the SMPs are still well constrained at the interface after passing through the structure at four right angles without introducing backscattering. This exclusive property is critical for designing optical devices with complex structures.

Conclusions The dispersion equation of the dielectric/gyro-electric model of the SMPs was theoretically analyzed, and the relationship requirement between the dielectric tensor and the dielectric coefficient was obtained, so as to achieve unidirectional transmission of the SMPs. According to the effective tensor theory, a meta-material with the combination of Ce∶YIG/Ag was proposed to construct a gyro-electric material, so as to satisfy the requirement. The dispersion

characteristics of the SMPs were analyzed, and the transmission characteristics were simulated by a finite element method. An SMPs-based unidirectional waveguide operating in the near-infrared band was constructed by two materials of Ce∶YIG/Ag with a magnetic field with normal magnitude (0.2 T). The unidirectional waveguide structure with defects was also simulated, and the results show that the SMPs-based unidirectional waveguide has good robustness.

Key words optics at surfaces; surface magnetoplasmons; unidirectional electromagnetic mode; meta-material; near-infrared; finite element method